

Inhibition of Interleukin 10 Transcription through the SMAD2/3 Signaling Pathway by Ca²⁺-Activated K⁺ Channel K_{Ca}3.1 Activation in Human T-Cell Lymphoma HuT-78 Cells[§]

Miki Matsui, Junko Kajikuri, Hiroaki Kito, Kyoko Endo, Yuki Hasegawa, Shinya Murate, and  Susumu Ohya

Department of Pharmacology, Kyoto Pharmaceutical University, Kyoto, Japan (M.M., K.E., Y.H.) and Department of Pharmacology, Graduate School of Medical Sciences, Nagoya City University, Nagoya, Japan (M.M., J.K., H.K., K.E., S.M., S.O.)

Received September 11, 2018; accepted January 6, 2019

ABSTRACT

The hyperpolarization induced by intermediate-conductance Ca²⁺-activated K⁺ channel (K_{Ca}3.1) activation increases the driving force for Ca²⁺ influx, which generally promotes cell proliferation, migration, and cytokine production in immunocompetent cells. Interleukin-10 (IL-10) from tumor-infiltrating lymphocytes and macrophages, lymphoma, and carcinoma cells facilitates escape from cancer immune surveillance; however, the role of K_{Ca}3.1 in IL-10 production remains unclear. The objective of the present study was to elucidate the involvement of K_{Ca}3.1 in IL-10 expression and production using the human T-cell lymphoma HuT-78 cells. In HuT-78 cells, IL-10 gene expression and production were reduced by treatment with the K_{Ca}3.1 activator, as 6-hour Western blotting showed that the protein expression ratio of phosphorylated Smad2 (P-Smad2)/Smad2, but not P-Smad3/Smad3, was decreased by the

treatment with K_{Ca}3.1 activator in HuT-78 cells. Concomitant with this, the nuclear translocation of P-Smad2 was inhibited by K_{Ca}3.1 activator. Furthermore, the K_{Ca}3.1 activator-induced transcriptional repression of IL-10 disappeared with pretreatment with the calmodulin kinase II (CaMKII) inhibitor KN-62 for 1 hour, and K_{Ca}3.1 activator-induced decreases in the nuclear translocation of P-Smad2 were also prevented by pretreatment with KN-62. Taken together, the K_{Ca}3.1 activator-induced transcriptional repression of IL-10 is due to the inhibition of the nuclear translocation of P-Smad2 in HuT-78 cells, resulting in the prevention of P-Smad2/3 complex formation in nuclei, and the activation of CaMKII induced by K_{Ca}3.1 activators suppresses the constitutive activation of P-Smad2/3 in HuT-78 cells. Therefore, K_{Ca}3.1 activators have potential as a therapeutic option to suppress the tumor-promoting activities of IL-10.

Introduction

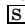
The anti-inflammatory cytokine interleukin-10 (IL-10) is an immunosuppressive factor involved in tumorigenesis and plays a crucial role in escape from cancer immune surveillance (Hamidullah et al., 2012). IL-10 expression is associated with lymphoproliferative disorders, such as lymphocytic leukemia, lymphoma, and myeloma (Benjamin et al., 1992; Finke et al., 1993; Lu et al., 1995). Increased IL-10 levels in patients with lymphoma are associated with poor survival due to the facilitation of tumor immune escape (Blay et al., 1993). IL-10 is frequently upregulated in various types of cancers (Sato et al., 2011), and the inhibition of IL-10 accelerates apoptosis in breast cancer cells (Alotaibi et al., 2018). The T-cell lymphoma cell line HuT-78, which is forkhead box P3

(Foxp3)/CD25-negative and constitutively produces IL-10, has been used to study the underlying mechanisms of IL-10 expression in T cells (Mori and Prager, 1997; Tiffon et al., 2011). Mori and Prager (1997) showed the involvement of the constitutive activation of nuclear factor- κ B (NF- κ B) in the high-level expression of IL-10 in HuT-78 cells. IL-10-producing naturally occurring regulatory T (T_{reg}) cells are Foxp3-positive CD4⁺CD25⁺ T cells and control autoimmunity (Itoh et al., 1999); however, recent studies showed that tumor-infiltrating Foxp3-negative CD4⁺CD25⁻ T cells are naturally present as IL-10-secreting T cells (Burugu et al., 2017; Ma et al., 2017).

Ca²⁺-activated K⁺ (K_{Ca}) channels are classified into three subfamilies based on their unitary conductance: K_{Ca}1.1, K_{Ca}2.x (2.1–2.3), and K_{Ca}3.1. In lymphoid and myeloid cells, membrane hyperpolarization by K⁺ channel opening (i.e., K_{Ca}3.1, voltage-gated K_V1.3, and two-pore domain K_{2P}5.1) increased the activity of Ca²⁺ release-activated Ca²⁺ channels and transient receptor potential Ca²⁺ channels (Cahalan and Chandy, 2009; Feske et al., 2015; Ohya and Kito, 2018).

This work was supported by JSPS KAKENHI [Grant JP16K08285] (S.O.). The authors declare no conflict of interest.

<https://doi.org/10.1124/mol.118.114405>

 This article has supplemental material available at molpharm.aspetjournals.org.

ABBREVIATIONS: AM, 2-acetoxymethyl ester; ACTB, β -actin; Blimp, B-lymphocyte-induced maturation protein; CaMK, Ca²⁺/calmodulin-dependent protein kinase; DCEBIO, 5,6-dichloro-1-ethyl-1,3-dihydro-2H-benzimidazol-2-one; E4BP, E4 promoter-binding protein; Foxp, forkhead box P; IFN, interferon; IL, interleukin; K_{Ca}, Ca²⁺-activated K⁺ (channel); mTOR, mammalian target of rapamycin; NDPK-B, nucleoside diphosphate kinase B; NF- κ B, nuclear factor- κ B; PCR, polymerase chain reaction; P-Smad, phosphorylated Smad; PI3K, phosphoinositide 3-kinase; STAT, signal transducers and activator of transcription; TGF, transforming growth factor; Th, helper T (cell).

Ca²⁺-dependent regulation of transcription factors [nuclear factor of activated T cells, NF- κ B, Ca²⁺/calmodulin-dependent protein kinase II (CaMKII), and mitogen-activated protein kinase] is involved in the activation of immune responses in T cells. K_{Ca}3.1 plays a pivotal role in the proliferation, differentiation, and migration of immune cells and is a potential therapeutic target for autoimmune and inflammatory disorders. In addition, the enhancement of K_{Ca}3.1 activity promotes proinflammatory cytokine production and secretion by regulating Ca²⁺ signaling in CD4⁺ T cells (Di et al., 2010; Ohya et al., 2014). In CD8⁺ T cells with the capacity to kill malignant cells, K⁺ efflux–mediating K_{Ca}3.1 activation increases antitumor function by promoting interferon (IFN)- γ production (Eil et al., 2016). The following positive and negative K_{Ca}3.1 function-modifying molecules have been identified in T cells: class II phosphoinositide 3-kinase B (PI3K-C2B), nucleoside diphosphate kinase B (NDPK-B), protein histidine phosphatase-1, phosphatidylinositol 3-phosphate myotubularin-related protein, phosphoglycerate mutase family member 5, and tripartite motif (family) 27 (Ohya and Kito, 2018). In T cells, K_{Ca}3.1 accumulates in the uropod, but not the leading edge, and is associated with oscillations in intracellular Ca²⁺ levels (Kuras et al., 2012). The pathologic significance of K_{Ca}3.1 in IL-10–producing T cells and cancerous cells remains to be elucidated.

Smad2 and Smad3 (Smad2/3) are essential transcription factors in the development and maintenance of T_{reg} cells (Sekiya et al., 2016). Phosphorylated Smad2/3 (P-Smad2/3) translocate to the nucleus, together with Smad4, and activate the transcription of downstream target genes (Derynck and Zhang, 2003). The constitutive activation of Smad2/3 signaling is evoked by constitutive transforming growth factor (TGF)- β signaling in resting human CD4⁺ T cells (Classen et al., 2007) and is maintained even in the presence of a TGF- β antagonist. CaMKII directly controls Smad2/3 function (Zimmerman et al., 1998; Wicks et al., 2000). The nuclear translocation of Smad2 is negatively regulated by Ca²⁺-dependent CaMKII signaling, which disrupts the P-Smad2/3 complex formation (Ming et al., 2010). Limited information is currently available on the role of Smad2/3 in proinflammatory and anti-inflammatory cytokine expression.

Herein, we examined the effects of K_{Ca}3.1 activators on the transcriptional repression of IL-10 in HuT-78 cells. Our results indicated that IL-10 is a downstream target gene of the Smad2/3 signaling pathway, and K_{Ca}3.1 activators inhibit the nuclear translocation of P-Smad2, which is constitutively active in HuT-78 cells. Our results also provide evidence for the importance of CaMKII signaling in the negative regulation of the nuclear translocation of Smad2 in HuT-78 cells.

Materials and Methods

Cell Culture. The human T-cell lymphoma cell line HuT-78 was supplied by the RIKEN BioResource Center (Tsukuba, Japan). The human leukemic T-cell lymphoblast cell line Jurkat clone E6, the human B lymphoma cell line Daudi, the human chronic myeloid leukemia cell line K562, and the human acute monocytic leukemia cell line THP-1 were supplied by the Japanese Collection of Research Bioresources Cell Bank (Osaka, Japan) and Cell Resource Center for Biomedical Research (Sendai, Japan). Cells were maintained at 37°C in 5% CO₂ with RPMI 1640 medium (Wako Pure Chemical Industries, Osaka, Japan) containing 10% fetal bovine serum (Sigma-Aldrich, St.

Louis, MO) and a penicillin-streptomycin mixture (Wako Pure Chemical Industries).

Real-Time Polymerase Chain Reaction Assay. Total RNA extraction and reverse transcription from HuT-78, Jurkat, Daudi, K562, and THP-1 cells were performed as previously reported (Endo et al., 2015). cDNA products were amplified with gene-specific polymerase chain reaction (PCR) primers, designated using Primer Express software (version 3.0.1; Thermo Fisher Scientific, Waltham, MA). Quantitative real-time PCR was performed using SYBR Green chemistry on an ABI 7500 Fast real-time PCR system (Thermo Fisher Scientific). The following gene-specific PCR primers of human origin were used for real-time PCR: K_{Ca}1.1 (GenBank accession number NM_001014797, 1120-1239), amplicon = 120 bp; K_{Ca}2.1 (NM_002248, 649-764), 116 bp; K_{Ca}2.2 (NM_021614, 1492-1612), 121 bp; K_{Ca}2.3 (NM_002249, 2042-2146), 105 bp; K_{Ca}3.1 (NM_002250, 1475-1595), 121 bp; NDPK-B (NM_002512, 288-408), 121 bp; PI3K-C2B (NM_002646, 4052-4172), 121 bp; protein histidine phosphatase-1 (NM_001135861, 783-903), 121 bp; phosphatidylinositol 3-phosphate myotubularin-related protein (NM_004685, 1476-1607), 132 bp; phosphoglycerate mutase family member 5 (NM_001170543, 277-396), 120 bp; tripartite motif (family) 27 (NM_006510, 1580-1702), 123 bp; IFN- γ (NM_000619, 403-522), 120 bp; IL-17A (NM_002190, 355-474), 120 bp; IL-4 (NM_000589, 287-406), 120 bp; IL-5 (NM_000879, 327-446), 120 bp; IL-13 (NM_002188, 166-285), 120 bp; IL-10 (NM_000572, 339-458), 120 bp; IL-32 (NM_001012631, 408-527), 120 bp; E4 promoter-binding protein (E4BP4; NM_001289999, 1217-1339), 123 bp; GATA3 (NM_001002295, 1335-1454), 120 bp; cMAF (NM_005360, 1697-1818), 120 bp; B-lymphocyte-induced maturation protein (Blimp1; NM_001198, 1425-1544), 120 bp; CD25 (NM_000417, 750-869), 120 bp; Foxp3 (NM_014009, 1253-1372), 120 bp; lymphocyte-activation gene-3 (NM_002286, 1289-1408), 120 bp; early growth response-2 (NM_000399, 590-711), 120 bp; and β -actin (ACTB) (NM_001101, 411-511), 101 bp. Unknown quantities relative to the standard curve for a particular set of primers were calculated as previously reported (Endo et al., 2015), yielding the transcriptional quantitation of gene products relative to the endogenous standard, ACTB.

Measurement of IL-10 Production by an Enzyme-Linked Immunosorbent Assay. Human IL-10 levels in culture supernatant samples were measured with a human IL-10 enzyme-linked immunosorbent assay kit (Thermo Fisher Scientific), according to the manufacturer's protocol. Six hours after the treatments with K_{Ca}3.1 activators, culture medium was exchanged with new medium, and an additional 18 hours after the treatments, culture supernatant samples were collected.

Western Blotting. Protein lysates were prepared from HuT-78 cells using radio-immunoprecipitation assay (RIPA) lysis buffer for Western blotting. Protein expression levels were measured 6 hours after the compound treatments. After the quantification of protein concentrations using the Bio-Rad DC protein assay, protein lysates were subjected to SDS-PAGE (10%). Blots were incubated with anti-Smad2/Smad3, P-Smad2 (Ser465/467), anti-P-Smad3 (Ser423/425; Cell Signaling Technology Japan, Tokyo, Japan), and anti-ACTB (Medical & Biologic Laboratories, Nagoya, Japan) antibodies, then incubated with anti-rabbit horseradish peroxidase-conjugated IgG (Merck, Darmstadt, Germany). An enhanced chemiluminescence detection system (Nacalai Tesque, Kyoto, Japan) was used to detect the bound antibody. The resulting images were analyzed using Amersham Imager 600 (GE Healthcare Japan, Tokyo, Japan). The light intensities of the Smad2/3, P-Smad2, and P-Smad3 protein band signals relative to that of the ACTB signal were calculated using ImageJ software (version 1.42; National Institutes of Health, Bethesda, MD), and the respective ratios of P-Smad2/Smad2 and P-Smad3/Smad3 were obtained. In summarized results, relative protein expression levels in the vehicle control were expressed as 1.0.

Measurement of Membrane Potential and Intracellular Ca²⁺ Concentrations by a Voltage-Sensitive Fluorescent Dye and Fluorescent Ca²⁺ Indicator Dye Imaging. Membrane potential was measured using the fluorescent voltage-sensitive dye DiBAC₄(3) as previously reported (Endo et al., 2015). Cells were seeded onto

fibronectin-coated glass-bottomed dishes (Matsunami, Osaka, Japan). In brief, prior to fluorescence measurements, HuT-78 cells were incubated in normal HEPES buffer containing 100 nM DiBAC₄(3) at room temperature for 20 minutes and then continuously incubated in 100 nM DiBAC₄(3) throughout the experiments. In addition, intracellular Ca²⁺ concentrations were measured using the fluorescent Ca²⁺ indicator dye Fura 2-acetoxymethyl ester (AM). Cells were incubated with 10 μM Fura 2-AM in normal HEPES solution for 30 minutes at room temperature. Cells loaded with Fura 2-AM were alternatively illuminated at wavelengths of 340 and 380 nm. Fluorescence images were recorded on the ORCA-Flash2.8 digital camera (Hamamatsu Photonics, Hamamatsu, Japan). Data collection and analyses were performed using an HCellImage system (Hamamatsu Photonics). Images were measured every 5 seconds.

Electrophysiological Recording. A whole-cell patch clamp was applied to single HuT-78 cells using the CEZ-2400 amplifier (Nihon Kohden, Tokyo, Japan) at room temperature (23°C ± 1°C). The procedures used for electrophysiological recordings and data acquisition/analysis have been reported previously (Ohya et al., 2014). Membrane potential values and whole-cell current densities were measured in the current- and voltage-clamp modes, respectively. Whole-cell currents were induced by ramp depolarization from -120 to +60 mV, 200 ms duration, every 15 seconds at +80 mV holding potential. The data were expressed as the current density (pA/pF). The external solution was as follows: 137 mM NaCl, 2.2 mM KCl, 1.2 mM MgCl₂, 14 mM glucose, and 10 mM HEPES (pH 7.4). The pipette solution was as follows: 140 mM KCl, 4 mM MgCl₂, 3.2 mM CaCl₂, 5 mM EGTA, 10 mM HEPES, and 2 mM Na₂ATP (pH 7.2), with an estimated free Ca²⁺ concentration of 300 nM (pCa 6.5).

Confocal Imaging of the Nuclear Translocation of P-Smad2 and P-Smad3. HuT-78 cells were fixed and permeabilized using the CytoFix/Perm kit (BD Pharmingen, Franklin Lakes, NJ). Anti-P-Smad2 and anti-P-Smad3 antibodies were labeled with an Alexa Fluor 488-conjugated secondary antibody (Abcam, Cambridge, UK), and nuclei were labeled with 4′6′-diamidino-2-phenylindole (DAPI). Fluorescence images were visualized using a confocal laser scanning microscope system (A1R; Nikon, Tokyo, Japan) (Endo et al., 2015). Image data were quantitatively analyzed using ImageJ software.

Chemicals. 5,6-Dichloro-1-ethyl-1,3-dihydro-2H-benzimidazol-2-one (DCEBIO, PubChem compound identifier 656765; Tocris Bioscience, Bristol, UK), SKA-31 (94880; Sigma-Aldrich), DiBAC₄(3) (6438341; Dojin, Kumamoto, Japan), LY364947 (447966; Cayman Chemical, Ann Arbor, MI), TRAM-34 (656734; Santa Cruz Biotechnology, Dallas, TX), KN-62 (5312126; MedChemexpress, Monmouth Junction, NJ), UCL1684 (656733; Tocris Bioscience), AZD 5363 (25227436; Cayman Chemical), 5,15-DPP (diphenylporphyrin, 10895852; Abcam), everolimus (6442177; Cayman Chemical), and Bay 11-7082 (535343; Sigma-Aldrich). The other chemicals used in the present study were from Sigma-Aldrich, Wako Pure Chemical Industries, or Nacalai Tesque unless otherwise stated.

Statistical Analysis. The significance of differences among two and multiple groups was evaluated using Student's *t* test and Tukey's test after the *F* test and analysis of variance, respectively. Significance at *P* < 0.05 and *P* < 0.01 is indicated in the figures. Data are presented as the means ± S.D.

Results

Functional Expression of K_{Ca}3.1 K⁺ Channels in IL-10-Expressing HuT-78 Cells. Previous studies showed that human T-cell lymphoma HuT-78 cells express the anti-inflammatory cytokine IL-10 at a relatively high level (Mori and Prager, 1997; Tiffon et al., 2011). HuT-78 cells strongly expressed IL-10 transcripts but not helper T 1 (Th1), Th2, or Th17 cytokine transcripts (IFN-γ, IL-17A, IL-4, IL-5, and IL-13) (Supplemental Fig. S1A), whereas the other hematologic cell lines (Jurkat E6, Daudi, K562, and THP-1) rarely

expressed IL-10 (Supplemental Fig. S1B). Concomitant with these results, IL-10 secretion was markedly higher in HuT-78 cells than in Jurkat E6, Daudi, K562, and THP-1 cells (Supplemental Fig. S1C). A quantitative PCR assay showed that HuT-78 cells negatively expressed CD25 and Foxp3 (Supplemental Fig. S1D). These results indicate that HuT-78 cells have a similar phenotype to CD4⁺CD25⁻Foxp3⁻ inducible regulatory T cells. IL-10-producing CD4⁺CD25⁻Foxp3⁻ inducible regulatory T cells express both the lymphocyte activation gene-3 and early growth response gene-2 (Okamura et al., 2009). HuT-78 cells expressed both genes at relatively high levels (Supplemental Fig. S1D).

Among five Ca²⁺-activated K⁺ channel subtypes, K_{Ca}3.1 transcripts were the most abundantly expressed in HuT-78 cells (Fig. 1A). Additionally, among six K_{Ca}3.1 function-modifying molecules, NDPK-B, which enhances K_{Ca}3.1 activity, was the most abundantly expressed in HuT-78 cells (Fig. 1B). The depolarization responses induced by the K_{Ca}3.1 inhibitor TRAM-34 (1 μM) were subsequently measured by voltage-sensitive fluorescent dye imaging. The application of TRAM-34 did not result in depolarization responses [*P* > 0.05 vs. vehicle control (0.1% dimethylsulfoxide)], suggesting that K_{Ca}3.1 is rarely activated under normal conditions in HuT-78 cells (Fig. 1, C and D). On the other hand, the application of two different K_{Ca}3.1 activators (1 μM DCEBIO and 1 μM SKA-31) induced hyperpolarization responses (*P* < 0.01 vs. vehicle control) (Fig. 1, C and D). An approximately 80% reduction in the DCEBIO-induced hyperpolarization response was observed following the application of 1 μM TRAM-34 (not shown). SKA-31 (1 μM)-induced activation of K_{Ca}3.1 was also observed using the whole-cell patch-clamp recordings. In current-clamp mode, the magnitude of membrane hyperpolarization by 1 μM SKA-31 was -69.6 ± 2.3 mV (*n* = 5, *P* < 0.01 vs. vehicle) (Supplemental Fig. S2, A and B). In voltage-clamp mode, the currents induced by ramp depolarization from -120 to +60 mV were activated by the application of 1 μM SKA-31 (Supplemental Fig. S2C), and the current density at +60 mV in SKA-31-treated cells (286.9 ± 97.6 pA/pF, *n* = 7, *P* < 0.05) was larger than the vehicle control (170.3 ± 95.0 pA/pF, *n* = 7) (Supplemental Fig. S2, C and D). Both SKA-31-induced hyperpolarization and current activation were suppressed following the application of 1 μM TRAM-34 (Supplemental Fig. S2, A and C). The application of K_{Ca}3.1 activators induced hyperpolarization-induced intracellular Ca²⁺ elevation (Fig. 1, E and F). The elevated Ca²⁺ levels (Δ ratio_{340/380}) were 0.017 ± 0.017 (*n* = 28), 0.063 ± 0.042 (*n* = 22, *P* < 0.01), and 0.052 ± 0.044 (*n* = 35, *P* < 0.01) in vehicle-, DCEBIO-, and SKA-31-treated cells, respectively.

Inhibitory Effects of K_{Ca}3.1 Activators on IL-10 Gene Expression and Production in HuT-78 Cells. Using IL-10-producing HuT-78 cells that functionally expressed K_{Ca}3.1 K⁺ channels, we examined the effects of K_{Ca}3.1 activators on IL-10 transcription and secretion. As shown in Fig. 2, A and C, IL-10 transcription and secretion were both reduced by treatments with 1 μM DCEBIO and 1 μM SKA-31. The expression levels of IL-10 transcripts relative to ACTB were 0.039 ± 0.002, 0.019 ± 0.002, and 0.025 ± 0.002 in vehicle-, DCEBIO-, and SKA-31-treated HuT-78 cells, respectively (*n* = 4 for each, *P* < 0.01 vs. vehicle control). The expression levels of vehicle-treated cells is arbitrarily expressed as 1.0. We further examined the effects of 30 mM

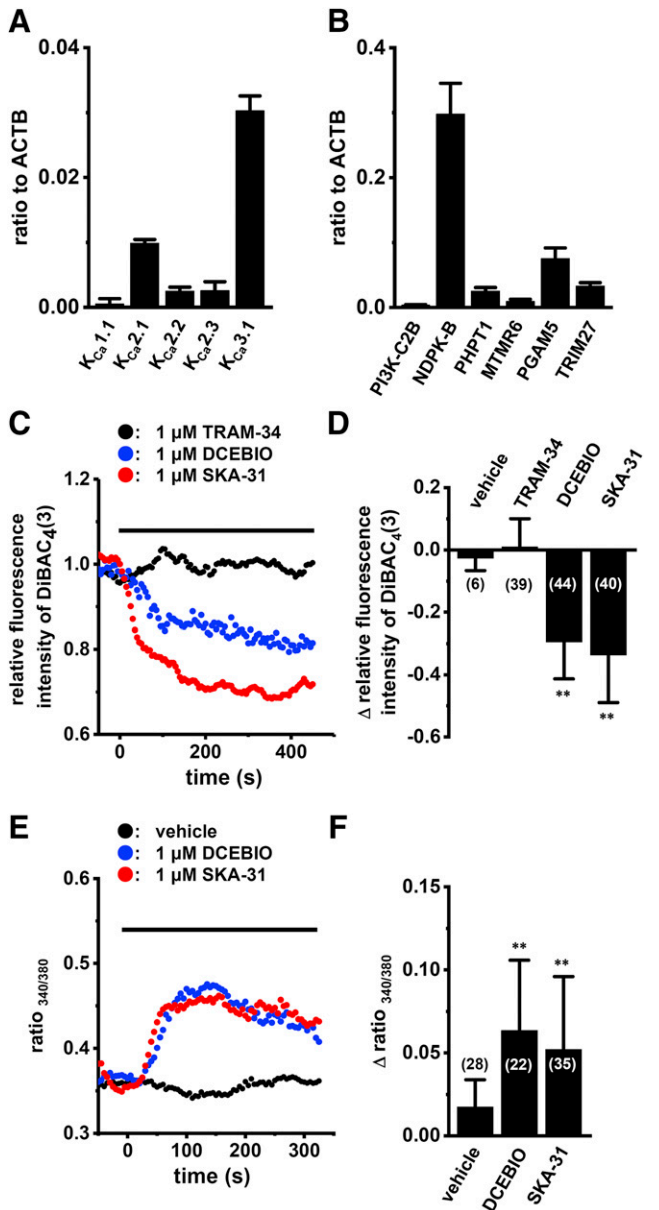


Fig. 1. Functional expression of K_{Ca}3.1 K⁺ channels in HuT-78 cells. (A and B) Real-time PCR assay for K_{Ca} channel subtypes (K_{Ca}1.1, K_{Ca}2.x, and K_{Ca}3.1) (A) and K_{Ca}3.1 function-modifying molecules [PI3K-C2B, NDPK-B, protein histidine phosphatase-1 (PHPT1), phosphatidylinositol 3-phosphate myotubularin-related protein (MTMR6), phosphoglycerate mutase family member 5 (PGAM5), and tripartite motif (family) 27 (TRIM27)] (B) (*n* = 4 for each). Expression levels were expressed as a ratio to ACTB. (C) The time course of changes in the relative fluorescent intensity of DiBAC₄(3) by the application of K_{Ca}3.1 activators (1 μM DCEBIO and 1 μM SKA-31) and a K_{Ca}3.1 inhibitor (1 μM TRAM-34). The fluorescent intensity of DiBAC₄(3) before the application of the agents at 0 seconds is expressed as 1.0. Horizontal bar shows the duration of drug application. (D) Summarized data are shown as Δ relative fluorescence intensity in vehicle (0.01% dimethylsulfoxide)-, TRAM-34-, DCEBIO-, and SKA-31-treated HuT-78 cells. (E) The time course of changes in the intracellular Ca²⁺ concentration ([Ca²⁺]_i) by the application of K_{Ca}3.1 activators. [Ca²⁺]_i was expressed as the Fura 2 ratio (340/380 nm). (F) Summarized data are shown as Δ Fura 2 ratio (340/380 nm) in vehicle-, DCEBIO-, and SKA-31-treated HuT-78 cells. Cell numbers used for the experiments are shown in parentheses. Results are expressed as means ± S.D. ***P* < 0.01 vs. vehicle control.

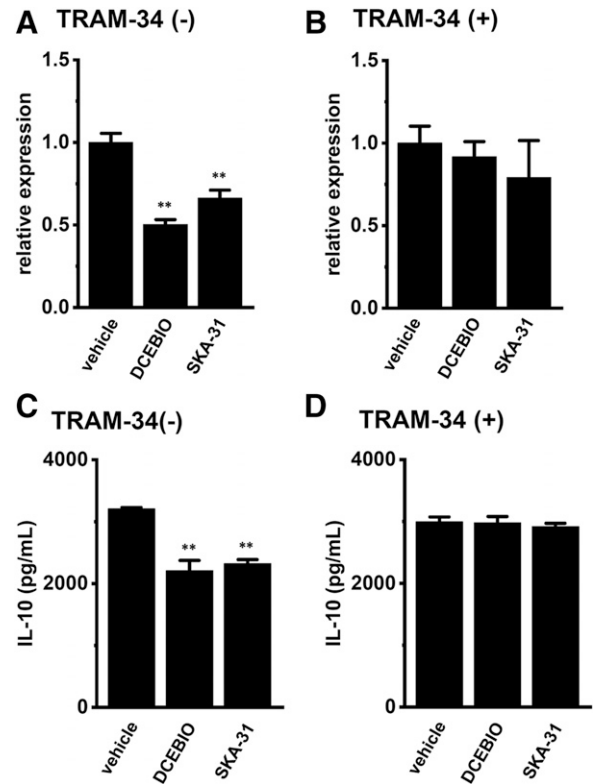


Fig. 2. Effects of treatments with K_{Ca}3.1 activators on IL-10 transcription and secretion in HuT-78 cells. (A and B) Quantitative real-time PCR assay for IL-10 in HuT-78 cells treated with vehicle, DCEBIO (1 μM), and SKA-31 (1 μM) for 6 hours in the absence [TRAM-34 (-)] and presence [TRAM-34 (+)] of 1 μM TRAM-34 (*n* = 4 for each). The expression level of vehicle-treated cells is arbitrarily expressed as 1.0, and data are shown as “relative expression.” (C and D) Quantitative detection of IL-10 by an enzyme-linked immunosorbent assay in HuT-78 cells treated with vehicle, DCEBIO, and SKA-31 for 18 hours (see *Materials and Methods*) in the absence (C) and presence (D) of TRAM-34. Results are expressed as means ± S.D. ***P* < 0.01 vs. vehicle control.

K⁺-induced depolarization on K_{Ca}3.1 activator-induced inhibition of IL-10 transcription in HuT-78 cells. The application of 30 mM K⁺-containing solution induced moderate depolarization in HuT-78 cells (Supplemental Fig. S3A). Similar to the results in Fig. 1C, 1 μM SKA-31 induced obvious hyperpolarization responses under normal K⁺ (2.2 mM) concentration; however, these responses almost disappeared with 30 mM K⁺-containing solution (Supplemental Fig. S3B). Concomitant with these results, K_{Ca}3.1 activator-induced inhibitions of IL-10 transcription disappeared by 30 mM K⁺-containing solution (Supplemental Fig. S3C). In addition, treatment with the Ca²⁺-ATPase inhibitor thapsigargin (1 nM) for 6 hours reduced IL-10 transcription (Supplemental Fig. S3D). IL-10 secretion levels (6–24 hours) were 3207 ± 22, 2206 ± 168, and 2321 ± 66 pg/ml in vehicle-, DCEBIO-, and SKA-31-treated HuT-78 cells, respectively (*n* = 4 for each, *P* < 0.01 vs. vehicle control) (Fig. 2C). Approximately 20% of IL-10 secretion was inhibited by treatments with K_{Ca}3.1 activators in HuT-78 cells. The transcriptional repression of IL-10 was not found 1 or 3 hours after treatments with K_{Ca}3.1 activators (Supplemental Fig. S4), and no changes in IL-10 secretion levels were observed in the culture medium from HuT-78 cells treated with vehicle, DCEBIO, and SKA-31 for 0–6 hours: 961 ± 62,

877 ± 114, and 872 ± 66 pg/ml, respectively ($n = 4$ for each, $P > 0.05$ vs. vehicle control). Consistent with the results shown in Fig. 2, C and D, no changes in the expression levels of IL-10 transcripts were noted following treatment with 1 μ M TRAM-34 for 6 hours: 0.038 ± 0.008 relative to ACTB ($n = 4$, $P > 0.05$ vs. vehicle control: 0.037 ± 0.004). When cells were co-treated with 1 μ M TRAM-34, reductions in IL-10 transcription and secretion by treatments with $K_{Ca}3.1$ activators were mostly prevented (Fig. 2, B and D). These results indicate that $K_{Ca}3.1$ is one of the molecules controlling IL-10 production in T-cell lymphoma.

Involvement of the Smad2/3 Signaling Pathway in $K_{Ca}3.1$ Activator-Induced Transcriptional Repression of IL-10 in HuT-78 Cells. As shown in Fig. 2A and Supplemental Fig. S4, B and C, IL-10 transcription was inhibited by $K_{Ca}3.1$ activation within 6 hours. These results suggest that the $K_{Ca}3.1$ activator-induced transcriptional repression of IL-10 is elicited through an IL-10 transcription factor-independent pathway. No changes in the transcriptional expression levels of the IL-10 transcription factors (E4BP4, GATA3, cMAF, and Blimp1) were found in HuT-78 cells (Fig. 3). Their expression levels relative to ACTB were 0.006 ± 0.001 , 0.080 ± 0.010 , 0.004 ± 0.001 , and 0.014 ± 0.004 , respectively, in vehicle-treated HuT-78 cells ($n = 4$ for

each). Kitani et al. (2003) showed that TGF- β 1/Smad signaling positively regulated IL-10 gene expression in Th1 cells. Therefore, we assessed the expression levels of P-Smad2 and P-Smad3 by Western blotting. As shown in Fig. 4A and Supplemental Fig. S5A, decreases in P-Smad2 proteins, but not P-Smad3, were found in $K_{Ca}3.1$ activator-treated (for 6 hours) HuT-78 cells without changes in total Smad2 and Smad3 protein expression. After the ratios of P-Smad2/3 to total Smad2/3 were calculated in vehicle-, DCEBIO-, and SKA-31-treated HuT-78 cells, those in the vehicle control were expressed as 1.0. The relative expression of P-Smad2, but not P-Smad3, in DCEBIO- and SKA-31-treated HuT-78 cells was reduced ($n = 5$ for each, $P < 0.01$) (Fig. 4, B and C). In addition, P-Smad2 and P-Smad3 proteins were expressed in vehicle-treated HuT-78 cells, suggesting that Smad2 and Smad3 are constitutively active and TGF- β 1-independently regulated in HuT-78 cells. The gene expression of IL-10 was not reduced by the treatment with the potent TGF- β 1 receptor blocker LY364947 (1 μ M) (Supplemental Fig. S6A).

To clarify whether $K_{Ca}3.1$ activators inhibit the nuclear translocation of P-Smad2 and/or P-Smad3 in HuT-78 cells, the cellular localization of P-Smad2/P-Smad3 was visualized by laser-scanning confocal fluorescence microscopy. Anti-P-Smad2 and anti-P-Smad3 antibodies were labeled with an Alexa Fluor 488-conjugated secondary antibody, and nuclei were labeled with 4'6'-diamidino-2-phenylindole (DAPI) (Fig. 5A). When the mean fluorescence intensities of the nuclear-cytoplasmic ratios of P-Smad2 and P-Smad3 were calculated, the nuclear translocation of P-Smad2, but not

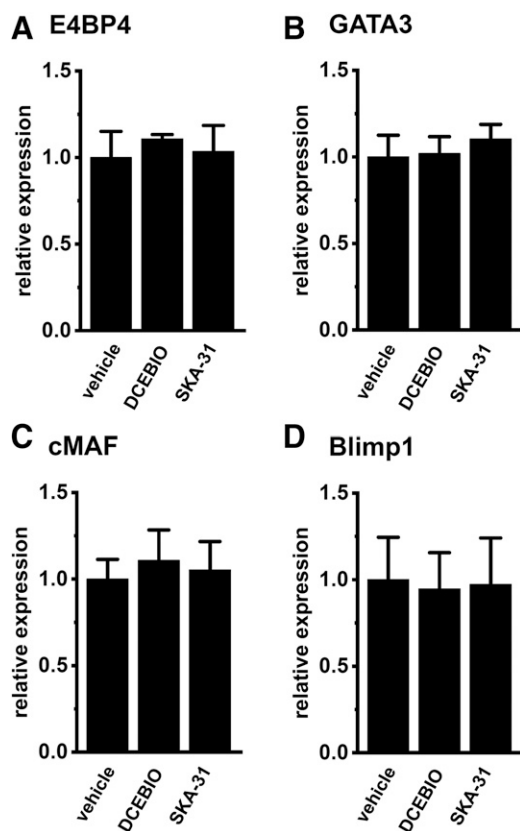


Fig. 3. Effects of treatments with $K_{Ca}3.1$ activators on the expression levels of transcription factors of IL-10 in HuT-78 cells. (A–D) Quantitative real-time PCR assay for transcription factors of IL-10 [E4BP4 (A), GATA3 (B), cMAF (C), and Blimp1 (D)] in HuT-78 cells treated with vehicle, DCEBIO (1 μ M), and SKA-31 (1 μ M) for 6 hours ($n = 4$ for each). The expression level of vehicle-treated cells is arbitrarily expressed as 1.0, and data are shown as “relative expression.” Results are expressed as means \pm S.D.

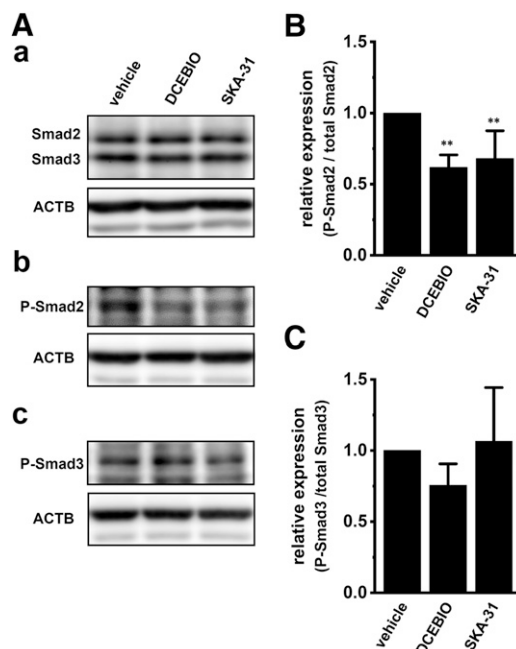


Fig. 4. Effects of treatments with $K_{Ca}3.1$ activators for 6 hours on the phosphorylation of Smad2 and Smad3 proteins in HuT-78 cells. (A) Whole protein lysates of DCEBIO (1 μ M)- and SKA-31 (1 μ M)-treated HuT-78 cells were probed by immunoblotting with anti-Smad2/Smad3 (a, upper panel), anti-P-Smad2 (b, upper panel), anti-P-Smad3 (c, upper panel), and anti-ACTB antibodies (a–c, lower panels). (B and C) Summarized results of the relative expression of P-Smad2/Smad2 and P-Smad3/Smad3 were obtained from the optical density of Smad2/3, P-Smad2, P-Smad3, and ACTB band signals ($n = 5$ for each) (see *Materials and Methods*). Results are expressed as means \pm S.D. ** $P < 0.01$ vs. vehicle control.

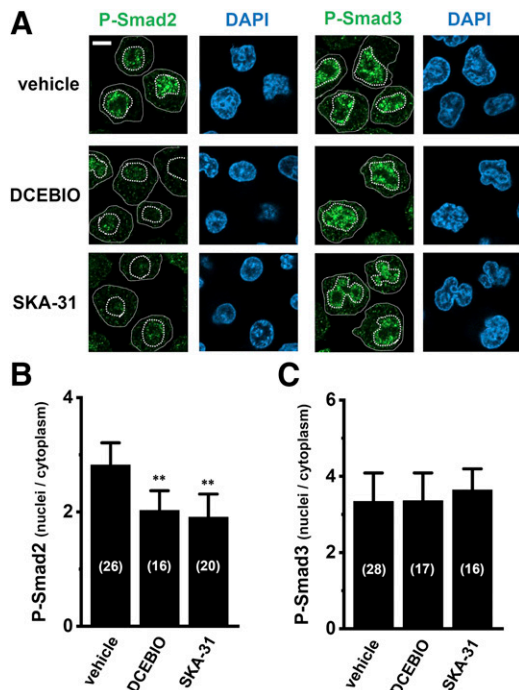


Fig. 5. Effects of treatments with K_{Ca}3.1 activators for 6 hours on the nuclear translocation of P-Smad2 and P-Smad3 in HuT-78 cells. (A) Confocal fluorescent images of Alexa Fluor 488-labeled P-Smad2 and P-Smad3 in vehicle-, DCEBIO (1 μ M)-, and SKA-31 (1 μ M)-treated HuT-78 cells. Nuclear morphologies were shown by 4'6'-diamidino-2-phenylindole (DAPI) images. Thick and thin dashed lines show the nuclear boundary and the plasma membrane, respectively. (B and C) Summarized results of the expression levels of P-Smad2 (B) and P-Smad3 (C) in the nuclei of HuT-78 cells. The mean fluorescent intensities of nuclear-cytoplasmic ratios were calculated. Results are expressed as means \pm S.D. Cell numbers used for the experiments are shown in parentheses. ** $P < 0.01$ vs. vehicle control.

P-Smad3, was reduced by treatments with K_{Ca}3.1 activators ($P < 0.01$) (Fig. 5, B and C). These results suggest that the nuclear translocation of P-Smad2 is regulated by the Ca²⁺-dependent K_{Ca}3.1 downstream signaling pathway(s), and thus, IL-10 as a target gene of Smad2/3 signaling may be transcriptionally regulated in HuT-78 cells.

Effects of the Ca²⁺/Calmodulin-Dependent Protein Kinase II Inhibitor on the K_{Ca}3.1 Activator-Induced Inhibition of IL-10 Expression and Secretion, P-Smad2 Protein Expression, and the Nuclear Translocation of P-Smad2 in HuT-78 Cells. CaMKII blocks the nuclear accumulation of Smad2 and prevents Smad2-Smad3 interactions (Zimmerman et al., 1998; Wicks et al., 2000). Increases in intracellular Ca²⁺ concentrations through K_{Ca}3.1 activation enhance the CaMKII signaling pathway. Therefore, we investigated whether pretreatment with the CaMKII inhibitor KN-62 (10 μ M) for 1 hour prevents: 1) K_{Ca}3.1 activator-induced inhibition of IL-10 transcription and secretion, 2) P-Smad2 protein expression, and 3) the nuclear translocation of P-Smad2 in HuT-78 cells. In Fig. 2, A and C, K_{Ca}3.1 activators inhibited IL-10 transcription and secretion. As shown in Fig. 6, the K_{Ca}3.1 activator-induced inhibition of IL-10 transcription and secretion disappeared following pretreatment with KN-62 in HuT-78 cells. The expression levels of IL-10 transcripts were 0.035 ± 0.004 , 0.040 ± 0.002 , and 0.040 ± 0.002 relative to ACTB in vehicle-, DCEBIO-, and SKA-31-treated groups, respectively ($n = 4$ for each, $P > 0.05$

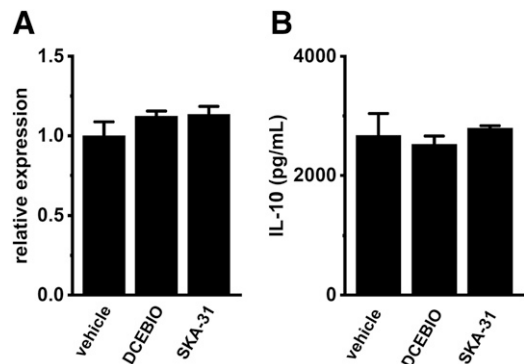


Fig. 6. Effects of the CaMKII inhibitor KN-62 (10 μ M) on K_{Ca}3.1 activator-induced reductions in IL-10 transcription and secretion in HuT-78 cells. (A) Quantitative real-time PCR assays for IL-10 in HuT-78 cells treated with vehicle, DCEBIO (1 μ M), and SKA-31 (1 μ M) for 6 hours in the presence of KN-62 ($n = 4$ for each). The expression level of vehicle-treated cells is arbitrarily expressed as 1.0, and data are shown as “relative expression.” (B) Quantitative detection of IL-10 by enzyme-linked immunosorbent assay assays in HuT-78 cells treated with vehicle, DCEBIO, and SKA-31 for 18 hours in the presence of KN-62. Results are expressed as means \pm S.D.

vs. vehicle control). Thapsigargin (1 nM)-induced inhibition of IL-10 transcription also disappeared following pretreatment with KN-62 (Supplemental Fig. S3D). In Figs. 4 and 5, K_{Ca}3.1 activators decreased the protein expression of P-Smad2 and the nuclear translocation of P-Smad2. K_{Ca}3.1 activator-induced decreases in the protein expression of P-Smad2 and the nuclear translocation of P-Smad2 were prevented by pretreatment with KN-62 in HuT-78 cells (Figs. 7 and 8; Supplemental Fig. S5B). These results suggest that CaMKII is an important mediator to promote the K_{Ca}3.1 activator-induced blockade of IL-10 transcription and secretion by suppressing the nuclear translocation of P-Smad2.

Discussion

The intermediate-conductance Ca²⁺-activated K⁺ channel K_{Ca}3.1 plays an important role in the control of proinflammatory cytokine production and secretion by regulating Ca²⁺ signaling in lymphoid and myeloid cells (Di et al., 2010; Ohya et al., 2014); however, it currently remains unclear whether K_{Ca}3.1 contributes to IL-10-induced escape from cancer immune surveillance. The present study showed that the pharmacological blockade of K_{Ca}3.1 by 1 μ M TRAM-34 did not evoke depolarization responses in human T-cell lymphoma HuT-78 cells under resting conditions (Fig. 1, C and D). These results suggest that K_{Ca}3.1 is rarely active under resting conditions in HuT-78 cells. In support of this hypothesis, IL-10 transcription was not affected by a single treatment with TRAM-34; however, TRAM-34 blocked K_{Ca}3.1 activator-induced decreases in IL-10 expression and secretion (Fig. 2, B and D). Using a whole-cell patch-clamp recording in current- and voltage-clamp modes, SKA-31-induced hyperpolarization and current activation were almost completely inhibited following the application of 1 μ M TRAM-34 (Supplemental Fig. S2). The main results of the present study are: 1) IL-10 expression and secretion were inhibited in HuT-78 cells treated with K_{Ca}3.1 activators (Fig. 2); 2) K_{Ca}3.1 activators reduced the phosphorylation of Smad2 and its nuclear translocation in HuT-78 cells (Figs. 4 and 5), resulting in the partial

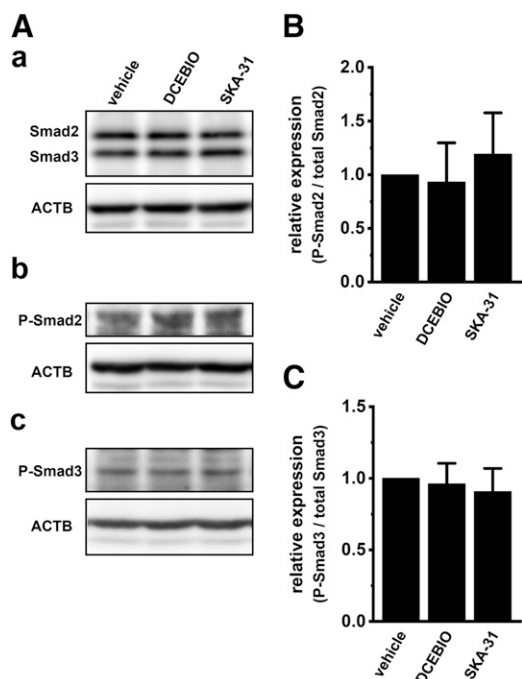


Fig. 7. Effects of the CaMKII inhibitor KN-62 (10 μ M) on $K_{Ca}3.1$ activator-induced reductions in the phosphorylation of Smad2 proteins in HuT-78 cells. (A) Whole protein lysates of DCEBIO (1 μ M)- and SKA-31 (1 μ M)-treated HuT-78 cells in the presence of KN-62 were probed by immunoblotting with anti-Smad2/Smad3 (a, upper panel), anti-P-Smad2 (b, upper panel), anti-P-Smad3 (c, upper panel), and anti-ACTB antibodies (a–c, lower panels). (B and C) Summarized results of the relative expression of P-Smad2/Smad2 and P-Smad3/Smad3 were obtained from the optical density of Smad2/3, P-Smad2, P-Smad3, and ACTB band signals ($n = 5$ for each). Results are expressed as means \pm S.D.

inhibition of constitutively active Smad2/3 signaling; and 3) the pharmacological inhibition of CaMKII signaling prevented the $K_{Ca}3.1$ activator-induced transcriptional repression of IL-10 through the reactivation of constitutively active Smad2/3 signaling (Figs. 6–8). This is the first evidence to suggest that $K_{Ca}3.1$ activators are a novel therapeutic option to suppress the tumor-promoting activities of IL-10 in escape from cancer immune surveillance.

During the last decade or two, several transcription factors of IL-10 have been identified in immune cells: E4BP4, GATA3, cMAF, and Blimp1 (Shoemaker et al., 2006; Motomura et al., 2011; Male et al., 2012; Heinemann et al., 2014; Rutz and Ouyang, 2016; Xu et al., 2018). As shown in Fig. 3, no changes in the expression levels of these transcripts by treatments with $K_{Ca}3.1$ activators for 6 hours were found in HuT-78 cells ($P > 0.05$). Priceman et al. (2006) reported that the expression level of E4BP4 was regulated in a Ca^{2+} -dependent manner in human leukemic cells; however, it was not affected by longer treatments with $K_{Ca}3.1$ activators for 12 and 24 hours (not shown). Alternatively, the proinflammatory cytokine IL-32, which is detected in sera from patients with Crohn's disease and rheumatoid arthritis, increases IL-10 transcription (Kang et al., 2009). In HuT-78 cells, IL-32 transcripts were expressed at a high level (approximately 10-fold that of IL-10); however, no changes were observed in their expression levels following treatments with $K_{Ca}3.1$ activators for 6 hours: 0.39 ± 0.02 , 0.48 ± 0.08 , and 0.40 ± 0.16 relative to ACTB in vehicle-, DCEBIO-, and SKA-31-treated HuT-78 cells, respectively ($n = 4$ for each, $P > 0.05$ vs. vehicle control). A recent study

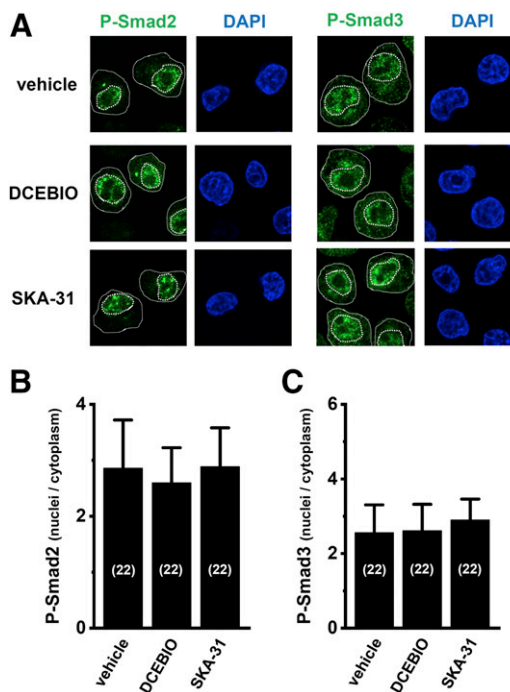


Fig. 8. Effects of the CaMKII inhibitor KN-62 (10 μ M) on $K_{Ca}3.1$ activator-induced reductions in the nuclear translocation of P-Smad2 in HuT-78 cells. (A) Confocal fluorescent images of Alexa Fluor 488-labeled P-Smad2 and P-Smad3 in vehicle-, DCEBIO (1 μ M)-, and SKA-31 (1 μ M)-treated HuT-78 cells in the presence of KN-62. Nuclear morphologies were shown by 4',6'-diamidino-2-phenylindole (DAPI) images. Thick and thin dashed lines show the nuclear boundary and plasma membrane, respectively. (B and C) Summarized results of the expression levels of P-Smad2 (B) and P-Smad3 (C) in the nuclei of HuT-78 cells. The mean fluorescent intensities of nuclear-cytoplasmic ratios were calculated. Results are expressed as means \pm S.D. Cell numbers used for the experiments are shown in parentheses.

showed that IL-10 transcription is epigenetically regulated in immune cells, and histone deacetylase 11 is a possible candidate for the transcriptional repression of IL-10 (Yanginlar and Logie, 2018). However, the expression levels of histone deacetylase 11 transcripts were extremely low in HuT-78 cells (less than 0.0001 relative to ACTB; not shown). These results suggest that these transcriptional and post-translational modulators are not involved in the $K_{Ca}3.1$ activator-induced transcriptional repression of IL-10.

Recent studies showed that $K_{Ca}3.1$ blockade attenuated pulmonary, renal, and corneal fibrosis by mediating Smad2/3 signaling (Huang et al., 2013, 2018; Roach and Wulff, 2014; Roach et al., 2015; Anumanthan et al., 2018). The resultant decreases in Ca^{2+} influx prevented the phosphorylation of Smad2/3 and nuclear translocation of P-Smad2/3 in fibroblasts, and thus, the expression levels of the downstream target genes (α -smooth muscle actin and collagen type I) were decreased. These results indicate that $K_{Ca}3.1$ is a “positive” regulator of Smad2/3 signaling in fibroblasts. In fibroblasts from patients with idiopathic pulmonary fibrosis, Ca^{2+} - and $K_{Ca}3.1$ -dependent processes contribute to the constitutive activation of Smad2/3 signaling (Roach et al., 2014, 2015). Mukherjee et al. (2017) showed that CaMKII activation did not affect Smad2/3 signaling in fibroblasts. However, the present study showed that $K_{Ca}3.1$ functioned as a “negative” regulator of Smad2/3 signaling through CaMKII in HuT-78 cells (Figs. 6–8). In HuT-78 cells, constitutively active NF- κ B

contributes to the constitutive facilitation of Smad2/3 signaling (Mori and Prager, 1997; Tiffon et al., 2011); however, resting K_{Ca}3.1 activity was very low (Fig. 1, C and D). Consistent with our results, previous studies reported that the inhibition of Smad2/3 signaling was strongly dependent on CaMKII activation, and CaMKII blocked the nuclear accumulation of Smad2 and prevented Smad2-Smad3 interactions (Zimmerman et al., 1998; Wicks et al., 2000). The present results provide novel evidence to suggest that K_{Ca}3.1 activators successfully inhibit constitutively active Smad2/3 signaling via CaMKII activation in IL-10-producing tumor-infiltrating lymphocytes and lymphoma.

Signal transducers and activator of transcription 3 (STAT3) and PI3K/AKT/mammalian target of rapamycin (mTOR) signaling pathways are both involved in the regulation of IL-10 expression (Braunschweig et al., 2011; Male et al., 2012; Zhu et al., 2015; Huang et al., 2016). STAT3 and mTOR inhibition reduced IL-10 expression in natural killer cells (Male et al., 2012) and peripheral dendritic cells (Weichhart et al., 2008), respectively. K_{Ca}3.1 blockade has been shown to inhibit the TGF- β 1 signaling pathway through PI3K/AKT/mTOR signaling pathways (Huang et al., 2016), whereas PI3K/AKT/mTOR signaling positively and negatively regulated STAT3 and NF- κ B, respectively (Weichhart et al., 2008). Furthermore, a positive feedback loop may operate to maintain strong STAT3 activity and IL-10 expression. IL-10 expression was reduced by treatment with the NF- κ B inhibitor Bay 11-7082 (1 μ M) (Supplemental Fig. S6B); however, no changes were observed in its expression following a treatment with the STAT3 inhibitor 5,15-DPP (20 μ M), the mTOR inhibitor everolimus (10 nM), and the AKT inhibitor AZD 5363 (1 μ M) for 6 (Supplemental Fig. S6C), 12, and 24 hours (not shown) in HuT-78 cells. These results suggest that STAT3 and PI3K/AKT/mTOR signaling pathways do not play an essential role in K_{Ca}3.1 activator-induced transcriptional repression in HuT-78 cells.

In conclusion, the present study provided a new approach to IL-10 regulation in cancer immunotherapy. The results obtained clearly showed that IL-10 is a downstream gene of Smad2/3 signaling in HuT-78 cells, and its production is negatively regulated by K_{Ca}3.1 activation, which blocks the nuclear accumulation of constitutively active Smad2 through CaMKII signaling. K_{Ca}3.1 activators are a possible therapeutic option to suppress the tumor-promoting activities of IL-10.

Acknowledgments

The authors sincerely thank Motoki Shimozaawa and Mayu Fujimoto for their technical assistance. Medical English Service (Kyoto, Japan) reviewed the manuscript prior to its submission.

Authorship Contributions

Participated in research design: Matsui, Ohya.

Conducted experiments: Matsui, Kajikuri, Kito, Endo, Hasegawa, Murate, Ohya.

Performed data analysis: Matsui, Kajikuri, Kito, Endo, Hasegawa, Murate, Ohya.

Wrote or contributed to the writing of the manuscript: Matsui, Kajikuri, Kito, Ohya.

References

Alotaibi MR, Hassan ZK, Al-Rejaie SS, Alshammari MA, Almutairi MM, Alhoshani AR, Alanazi WA, Hafez MM, and Al-Shabanah OA (2018) Characterization of apoptosis in a breast cancer cell line after IL-10 silencing. *Asian Pac J Cancer Prev* 19:777–783.

Anumanthan G, Gupta S, Fink MK, Hesemann NP, Bowles DK, McDaniel LM, Muhammad M, and Mohan RR (2018) K_{Ca}3.1 ion channel: a novel therapeutic target for corneal fibrosis. *PLoS One* 13:e0192145.

Benjamin D, Knobloch TJ, and Dayton MA (1992) Human B-cell interleukin-10: B-cell lines derived from patients with acquired immunodeficiency syndrome and Burkitt's lymphoma constitutively secrete large quantities of interleukin-10. *Blood* 80:1289–1298.

Blay JY, Burdin N, Rousset F, Lenoir G, Biron P, Philip T, Banchereau J, and Favrot MC (1993) Serum interleukin-10 in non-Hodgkin's lymphoma: a prognostic factor. *Blood* 82:2169–2174.

Braunschweig A, Poehlmann TG, Busch S, Schleussner E, and Markert UR (2011) Signal transducer and activator of transcription 3 (STAT3) and suppressor of cytokine signaling (SOCS3) balance controls cytotoxicity and IL-10 expression in decidual-like natural killer cell line NK-92. *Am J Reprod Immunol* 66:329–335.

Burugu S, Gao D, Leung S, Chia SK, and Nielsen TO (2017) LAG-3⁺ tumor infiltrating lymphocytes in breast cancer: clinical correlates and association with PD-1/PD-L1⁺ tumors. *Ann Oncol* 28:2977–2984.

Cahalan MD and Chandy KG (2009) The functional network of ion channels in T lymphocytes. *Immunol Rev* 231:59–87.

Classen S, Zander T, Eggle D, Chemnitz JM, Brors B, Büchmann I, Popov A, Beyer M, Eils R, Debey S, et al. (2007) Human resting CD4⁺ T cells are constitutively inhibited by TGF- β under steady-state conditions. *J Immunol* 178:6931–6940.

Derynck R and Zhang YE (2003) Smad-dependent and Smad-independent pathways in TGF- β family signalling. *Nature* 425:577–584.

Di L, Srivastava S, Zhdanova O, Ding Y, Li Z, Wulff H, Lafaille M, and Skolnik EY (2010) Inhibition of the K⁺ channel K_{Ca}3.1 ameliorates T cell-mediated colitis. *Proc Natl Acad Sci USA* 107:1541–1546.

Eil R, Vodnala SK, Clever D, Klebanoff CA, Sukumar M, Pan JH, Palmer DC, Gros A, Yamamoto TN, Patel SJ, et al. (2016) Ionic immune suppression within the tumour microenvironment limits T cell effector function. *Nature* 537:539–543.

Endo K, Kurokawa N, Kito H, Nakakura S, Fujii M, and Ohya S (2015) Molecular identification of the dominant-negative, splicing isoform of the two-pore domain K⁺ channel K_{Ca}3.1 in lymphoid cells and enhancement of its expression by splicing inhibition. *Biochem Pharmacol* 98:440–452.

Feske S, Wulff H, and Skolnik EY (2015) Ion channels in innate and adaptive immunity. *Annu Rev Immunol* 33:291–353.

Finke J, Ternes P, Lange W, Mertelsmann R, and Dölken G (1993) Expression of interleukin 10 in B lymphocytes of different origin. *Leukemia* 7:1852–1857.

Hamidullah CB, Changkija B, and Konwar R (2012) Role of interleukin-10 in breast cancer. *Breast Cancer Res Treat* 133:11–21.

Heinemann C, Heink S, Petermann F, Vasanthakumari A, Rothhammer V, Doorduyn E, Mitsdoerffer M, Sie C, Prazeres da Costa O, Buch T, et al. (2014) IL-27 and IL-12 oppose pro-inflammatory IL-23 in CD4⁺ T cells by inducing Blimp1. *Nat Commun* 5:3770.

Huang C, Lin MZ, Cheng D, Braet F, Pollock CA, and Chen XM (2016) K_{Ca}3.1 mediates dysfunction of tubular autophagy in diabetic kidneys via PI3K/Akt/mTOR signaling pathways. *Sci Rep* 6:23884.

Huang C, Shen S, Ma Q, Chen J, Gill A, Pollock CA, and Chen XM (2013) Blockade of K_{Ca}3.1 ameliorates renal fibrosis through the TGF- β 1/Smad pathway in diabetic mice. *Diabetes* 62:2923–2934.

Huang C, Zhang L, Shi Y, Yi H, Zhao Y, Chen J, Pollock CA, and Chen XM (2018) The K_{Ca}3.1 blocker TRAM34 reverses renal damage in a mouse model of established diabetic nephropathy. *PLoS One* 13:e0192800.

Itoh M, Takahashi T, Sakaguchi N, Kuniyasu Y, Shimizu J, Otsuka F, and Sakaguchi S (1999) Thymus and autoimmunity: production of CD25⁺CD4⁺ naturally anergic and suppressive T cells as a key function of the thymus in maintaining immunologic self-tolerance. *J Immunol* 162:5317–5326.

Kang JW, Choi SC, Cho MC, Kim HJ, Kim JH, Lim JS, Kim SH, Han JY, and Yoon DY (2009) A proinflammatory cytokine interleukin-32 β promotes the production of an anti-inflammatory cytokine interleukin-10. *Immunology* 128(1 Suppl): e532–e540.

Kitani A, Fuss I, Nakamura K, Kumaki F, Usui T, and Strober W (2003) Transforming growth factor (TGF)- β 1-producing regulatory T cells induce Smad-mediated interleukin 10 secretion that facilitates coordinated immunoregulatory activity and amelioration of TGF- β 1-mediated fibrosis. *J Exp Med* 198:1179–1188.

Kuras Z, Yun YH, Chimote AA, Neumeier L, and Conforti L (2012) K_{Ca}3.1 and TRPM7 channels at the uropod regulate migration of activated human T cells. *PLoS One* 7:e43859.

Lu ZY, Zhang XG, Rodriguez C, Wijdenes J, Gu ZJ, Morel-Fournier B, Harousseau JL, Bataille R, Rossi JF, and Klein B (1995) Interleukin-10 is a proliferation factor but not a differentiation factor for human myeloma cells. *Blood* 85:2521–2527.

Ma QY, Huang DY, Zhang HJ, Wang S, and Chen XF (2017) Function and regulation of LAG3 on CD4⁺CD25⁺ T cells in non-small cell lung cancer. *Exp Cell Res* 360: 358–364.

Male V, Nisoli I, Gascoyne DM, and Brady HJ (2012) E4BP4: an unexpected player in the immune response. *Trends Immunol* 33:98–102.

Ming M, Manzini I, Le W, Krieglstein K, and Spittau B (2010) Thapsigargin-induced Ca²⁺ increase inhibits TGF β 1-mediated Smad2 transcriptional responses via Ca²⁺/calmodulin-dependent protein kinase II. *J Cell Biochem* 111:1222–1230.

Mori N and Prager D (1997) Activation of the interleukin-10 gene in the human T lymphoma line HuT 78: identification and characterization of NF- κ B binding sites in the regulatory region of the interleukin-10 gene. *Eur J Haematol* 59:162–170.

Motomura Y, Kitamura H, Hijikata A, Matsunaga Y, Matsumoto K, Inoue H, Atarashi K, Hori S, Watarai H, Zhu J, et al. (2011) The transcription factor E4BP4 regulates the production of IL-10 and IL-13 in CD4⁺ T cells. *Nat Immunol* 12: 450–459.

Mukherjee S, Sheng W, Sun R, and Janssen LJ (2017) Ca²⁺/calmodulin-dependent protein kinase II β and II δ mediate TGF β -induced transduction of fibronectin and collagen in human pulmonary fibroblasts. *Am J Physiol Lung Cell Mol Physiol* 312: L510–L519.

- Ohya S, Fukuyo Y, Kito H, Shibaoka R, Matsui M, Niguma H, Maeda Y, Yamamura H, Fujii M, Kimura K, et al. (2014) Upregulation of KCa3.1 K(+) channel in mesenteric lymph node CD4(+) T lymphocytes from a mouse model of dextran sodium sulfate-induced inflammatory bowel disease. *Am J Physiol Gastrointest Liver Physiol* **306**:G873–G885.
- Ohya S and Kito H (2018) Ca²⁺-activated K⁺ channel KCa3.1 as a therapeutic target for immune disorders. *Biol Pharm Bull* **41**:1158–1163.
- Okamura T, Fujio K, Shibuya M, Sumitomo S, Shoda H, Sakaguchi S, and Yamamoto K (2009) CD4⁺CD25⁺LAG3⁺ regulatory T cells controlled by the transcription factor Egr-2. *Proc Natl Acad Sci USA* **106**:13974–13979.
- Priceman SJ, Kirzner JD, Nary LJ, Morris D, Shankar DB, Sakamoto KM, and Medh RD (2006) Calcium-dependent upregulation of E4BP4 expression correlates with glucocorticoid-evoked apoptosis of human leukemic CEM cells. *Biochem Biophys Res Commun* **344**:491–499.
- Roach KM, Feghali-Bostwick C, Wulff H, Amrani Y, and Bradding P (2015) Human lung myofibroblast TGFβ1-dependent Smad2/3 signalling is Ca(2+)-dependent and regulated by KCa3.1 K(+) channels. *Fibrogenesis Tissue Repair* **8**:5.
- Roach KM, Wulff H, Feghali-Bostwick C, Amrani Y, and Bradding P (2014) Increased constitutive αSMA and Smad2/3 expression in idiopathic pulmonary fibrosis myofibroblasts is KCa3.1-dependent. *Respir Res* **15**:155.
- Rutz S and Ouyang W (2016) Regulation of interleukin-10 expression. *Adv Exp Med Biol* **941**:89–116.
- Sato T, Terai M, Tamura Y, Alexeev V, Mastrangelo MJ, and Selvan SR (2011) Interleukin 10 in the tumor microenvironment: a target for anticancer immunotherapy. *Immunol Res* **51**:170–182.
- Sekiya T, Nakatsukasa H, Lu Q, and Yoshimura A (2016) Roles of transcription factors and epigenetic modifications in differentiation and maintenance of regulatory T cells. *Microbes Infect* **18**:378–386.
- Shoemaker J, Saraiva M, and O'Garra A (2006) GATA-3 directly remodels the IL-10 locus independently of IL-4 in CD4⁺ T cells. *J Immunol* **176**:3470–3479.
- Tiffon C, Adams J, van der Fits L, Wen S, Townsend P, Ganesan A, Hodges E, Vermeer M, and Packham G (2011) The histone deacetylase inhibitors vorinostat and romidepsin downmodulate IL-10 expression in cutaneous T-cell lymphoma cells. *Br J Pharmacol* **162**:1590–1602.
- Weichhart T, Costantino G, Poglitsch M, Rosner M, Zeyda M, Stuhlmeier KM, Kolbe T, Stulnig TM, Hörl WH, Hengstschläger M, et al. (2008) The TSC-mTOR signaling pathway regulates the innate inflammatory response. *Immunity* **29**:565–577.
- Wicks SJ, Lui S, Abdel-Wahab N, Mason RM, and Chantray A (2000) Inactivation of smad-transforming growth factor beta signaling by Ca²⁺-calmodulin-dependent protein kinase II. *Mol Cell Biol* **20**:8103–8111.
- Xu M, Pokrovskii M, Ding Y, Yi R, Au C, Harrison OJ, Galan C, Belkaid Y, Bonneau R, and Littman DR (2018) c-MAF-dependent regulatory T cells mediate immunological tolerance to a gut pathobiont. *Nature* **554**:373–377.
- Yanginlar C and Logie C (2018) HDAC11 is a regulator of diverse immune functions. *Biochim Biophys Acta Gene Regul Mech* **1861**:54–59.
- Zhu YP, Brown JR, Sag D, Zhang L, and Suttles J (2015) Adenosine 5'-monophosphate-activated protein kinase regulates IL-10-mediated anti-inflammatory signaling pathways in macrophages. *J Immunol* **194**:584–594.
- Zimmerman CM, Kariapper MST, and Mathews LS (1998) Smad proteins physically interact with calmodulin. *J Biol Chem* **273**:677–680.

Address correspondence to: Dr. Susumu Ohya, Department of Pharmacology, Graduate School of Medical Sciences, Nagoya City University, Nagoya 467-8601, Japan. E-mail: sohya@med.nagoya-cu.ac.jp

Article's title: Inhibition of interleukin 10 transcription through the SMAD2/3 signaling pathway by Ca²⁺-activated K⁺ channel K_{Ca}3.1 activation in human T-cell lymphoma HuT-78 cells

Authors: Miki Matsui, Junko Kajikuri, Hiroaki Kito, Kyoko Endo, Yuki Hasegawa, Shinya Murate, Susumu Ohya

Journal title: Molecular Pharmacology (MOL # 114405)

Supplementary Figure legends

Figure S1. Gene expression of Th1 and Th2 cytokines, CD25, Foxp3, LAG3, and EGR2 in HuT-78 cells and differential levels of IL-10 expression and secretion in HuT-78, Jurkat, Daudi, K562, and THP-1 cells. A: Quantitative real-time PCR assay for IFN- γ , IL-17A, IL-4, IL-5, and IL-13 in HuT-78 cells (n=4). Expression levels were shown as a ratio to ACTB. B: Real-time PCR assay for IL-10 in HuT-78, Jurkat, Daudi, K562, and THP-1 cells (n=4 for each). C: Quantitative detection of IL-10 by ELISA assays in HuT-78, Jurkat, Daudi, K562, and THP-1 cells (n=4 for each). Supernatant samples were collected 24 hr after cultivation. D: Real-time PCR assays for CD25, Foxp3, LAG3, and EGR2 in HuT-78 cells (n=4). Results are expressed as means \pm S.D.

Figure S2. The SKA-31-induced hyperpolarization and current activation in HuT-78 cells in current- and voltage-clamp mode using whole-cell patch clamp recordings (at pCa 6.5). A: The time course of hyperpolarization responses induced by the application of 1 μ M SKA-31. B: Summarized results of the changes in membrane potential was obtained from 'A' (n=5 for each). C: Effects of vehicle (black), 1 μ M SKA-31 (red) and 1 μ M SKA-31 + 1 μ M TRAM-34 (blue) on the current density-voltage relationship for voltage ramp-induced currents from -120 to +60 mV in HuT-78 cells. D: Summarized results of 1 μ M SKA-31-induced outward current density at +60 mV (n=7 for each). Results are expressed as means \pm S.D. *, **: $P < 0.05, 0.01$ vs. vehicle control,

Figure S3. Effects of 30 mM K⁺-containing solution and 1 nM thapsigargin on K_{Ca}3.1 activators-induced inhibition of IL-10 transcription in HuT-78 cells. A: The time course of depolarization responses induced by the application of 30 and 140 mM K⁺-containing solution.

The fluorescent intensity of DiBAC₄(3) before the application of the agents at 0 sec is expressed as 1.0. B: Disappearance of 1 μ M SKA-31-induced hyperpolarization responses by the application of 30 mM K⁺-containing solution. Cell numbers used for the experiments are shown in parentheses. C: Quantitative real-time PCR assay for IL-10 in HuT-78 cells treated with vehicle, DCEBIO (1 μ M), DCEBIO + 30 mM K⁺, SKA-31 (1 μ M), and SKA-31 + 30 mM K⁺ for 6 hr (n=4 for each). D: Real-time PCR assay for IL-10 in HuT-78 cells treated with vehicle, 1 nM thapsigargin (TG), and TG + 10 μ M KN-62 for 6 hr (n=4 for each). Expression levels were expressed as a ratio to ACTB. Results are expressed as means \pm S.D. **: $P < 0.01$ vs. vehicle control, #: $P < 0.01$ vs. DCEBIO-treated, \$\$: $P < 0.01$ vs. SKA-31-treated, ¶: $P < 0.01$ vs. TG-treated.

Figure S4. Time course of decreases in IL-10 transcripts by treatments with K_{Ca}3.1 activators in HuT-78 cells. A-C: Quantitative real-time PCR assay for IL-10 in HuT-78 cells treated with vehicle (A), DCEBIO (1 μ M) (B), and SKA-31 (1 μ M) (C) for 1, 3, 6, 12, and 24 hr (n=4 for each). Expression levels were expressed as a ratio to ACTB. Results are expressed as means \pm S.D. **: $P < 0.01$ vs. at 0 hr.

Figure S5. Full images of cropped blots in Figure 4 (A) and Figure 7 (A)

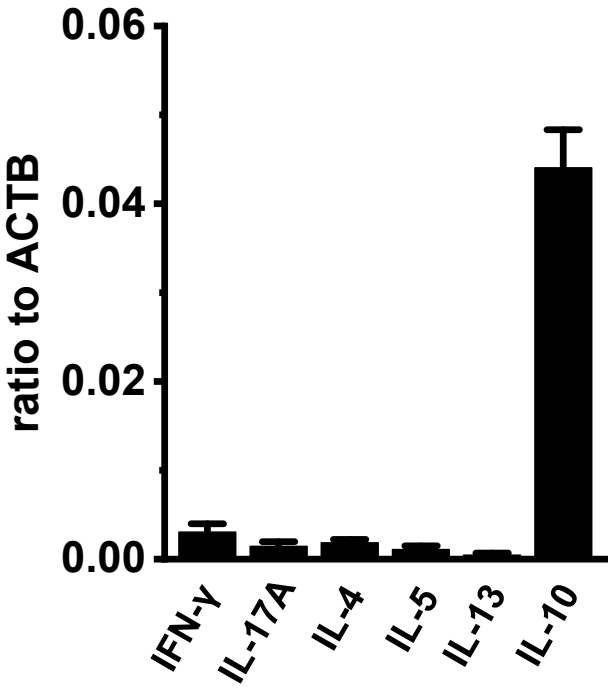
Figure S6. Effects of an ATP competitive inhibitor of the TGF- β 1 receptor (LY364947), NF- κ B inhibitor (BAY11-7082), mTOR inhibitor (everolimus), AKT inhibitor (AZD5363), and STAT3 inhibitor (5,15-DPP) on expression levels of IL-10 transcripts in HuT-78 cells. A-C: Quantitative real-time PCR assay for IL-10 in HuT-78 cells treated with vehicle, LY364947 (1 μ M) (A), BAY11-7082 (1 μ M) (B), everolimus (10 nM) (C), AZD5363 (1 μ M) (C), and 5,15-

DPP (20 μ M) (C) for 6 hr (n=4 for each). Expression levels were expressed as a ratio to ACTB.

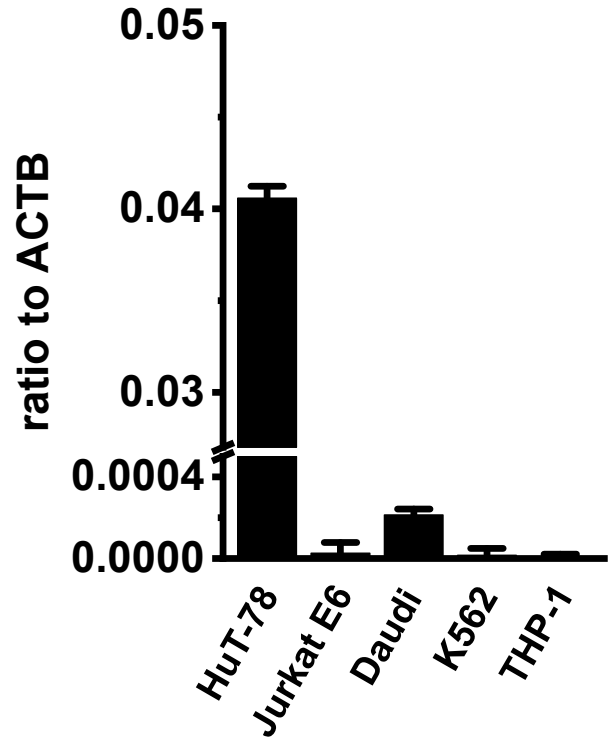
Results are expressed as means \pm S.D. **: $P < 0.01$ vs. vehicle control.

supplementary Fig. S1

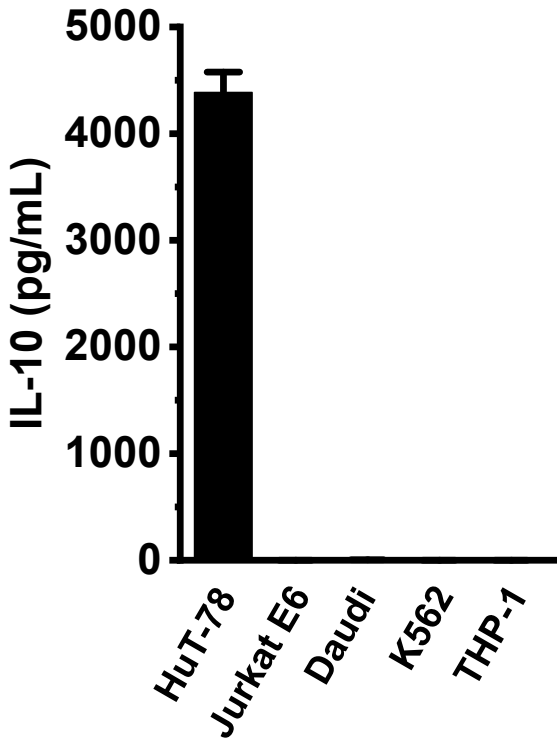
A



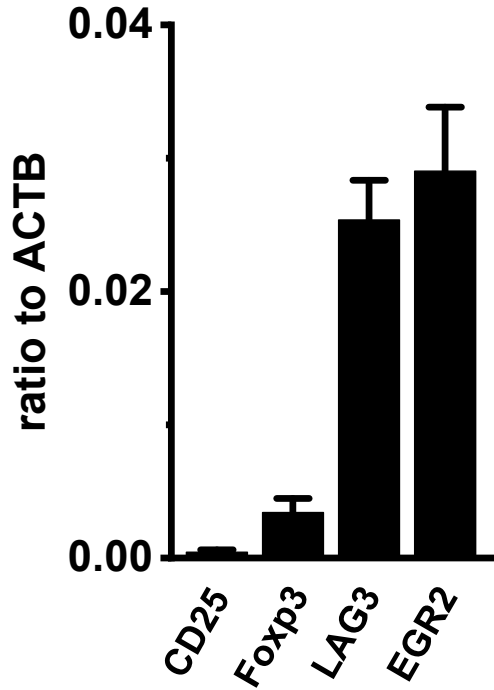
B



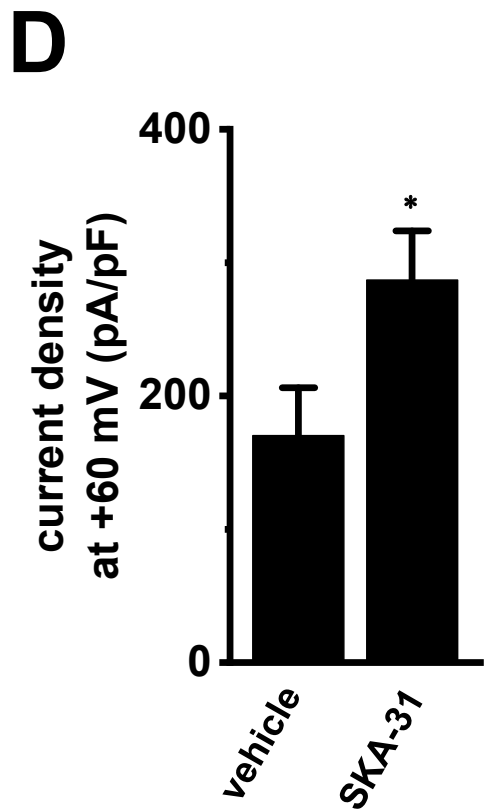
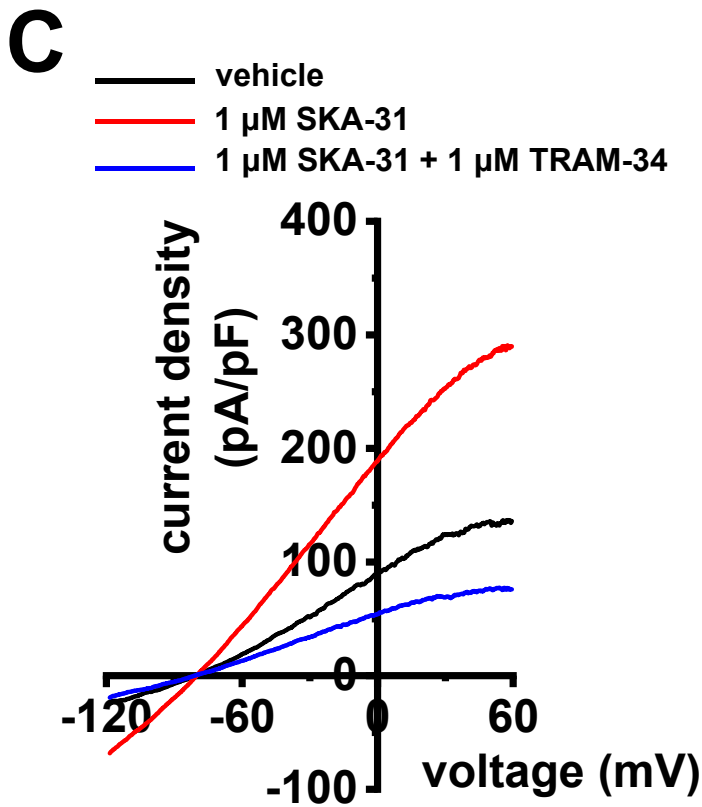
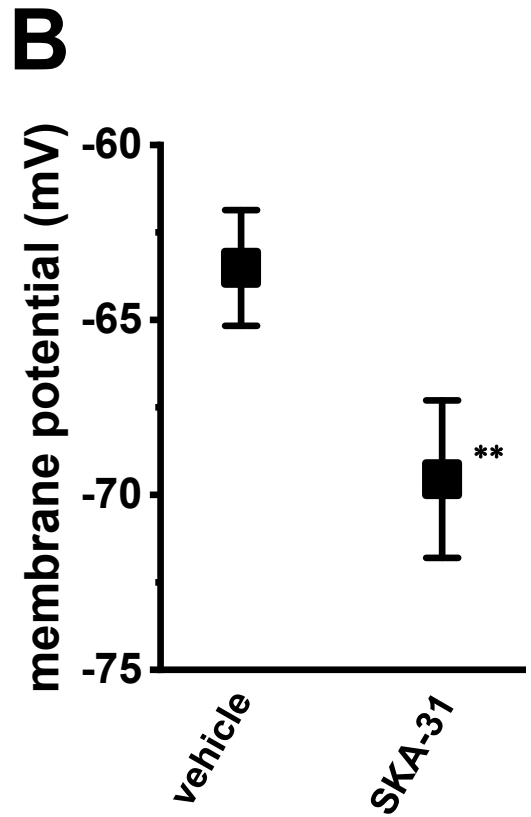
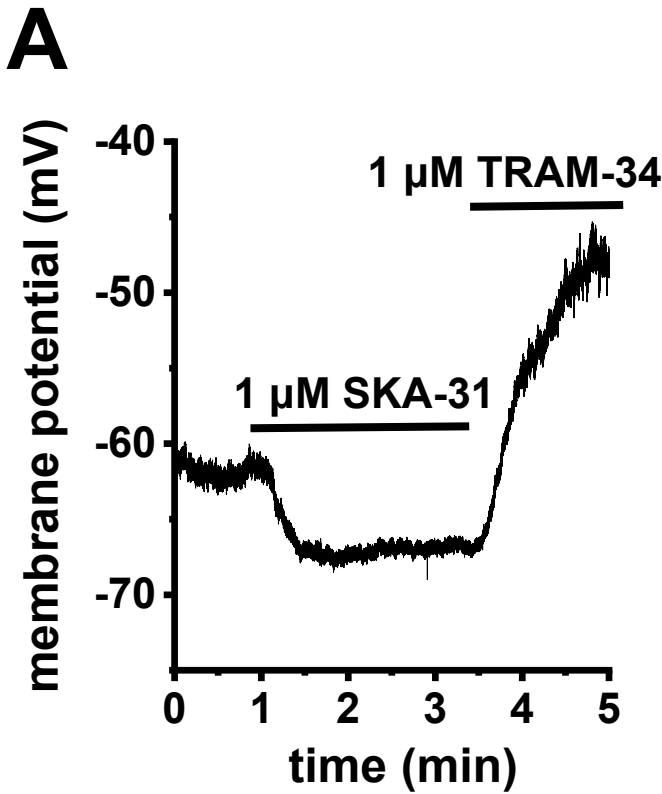
C



D

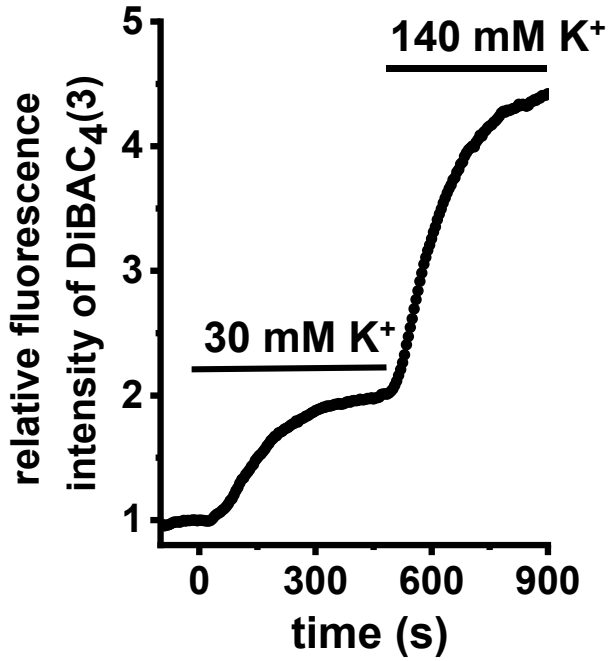


supplementary Fig. S2

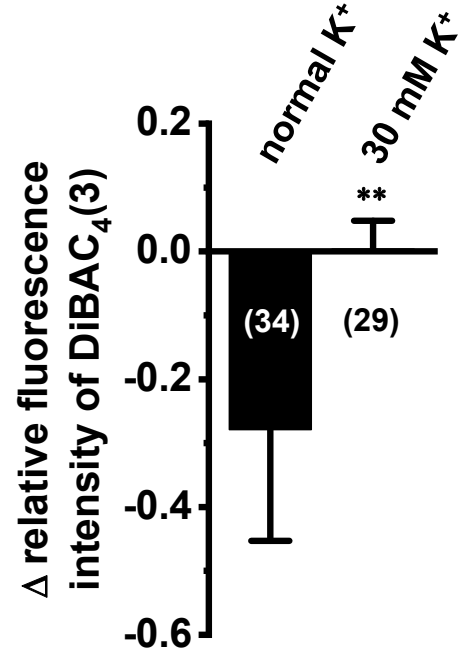


supplementary Fig. S3

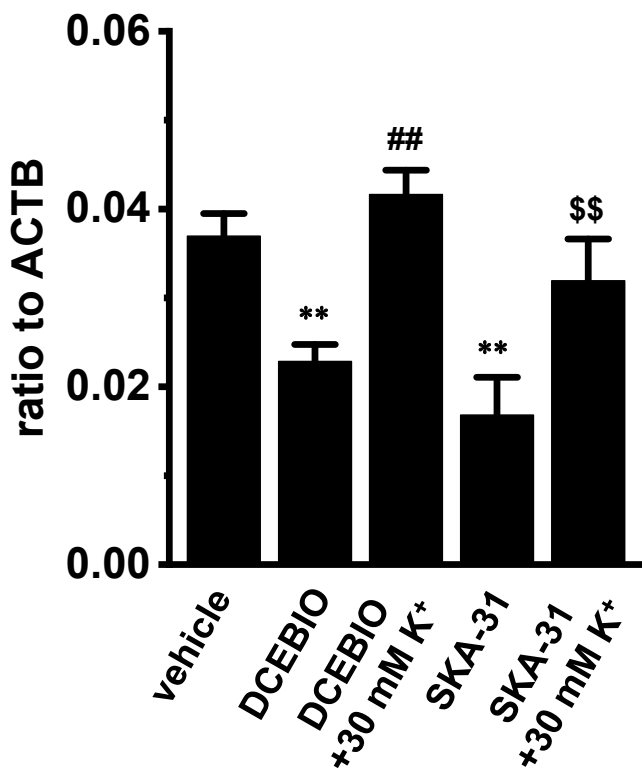
A



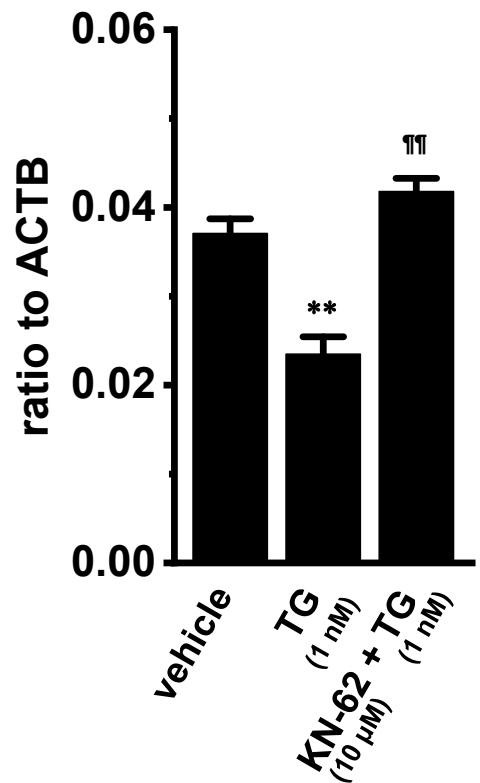
B



C

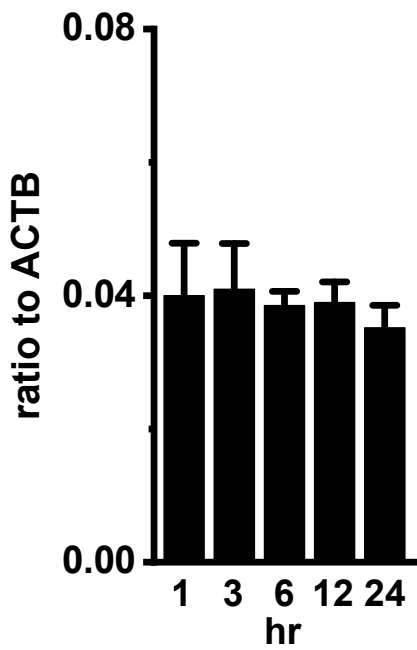


D

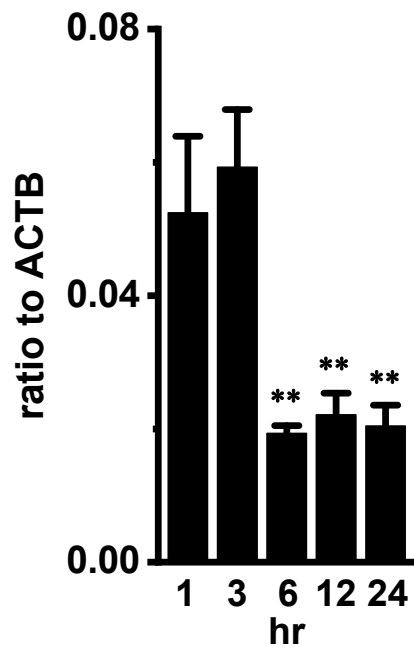


supplementary Fig. S4

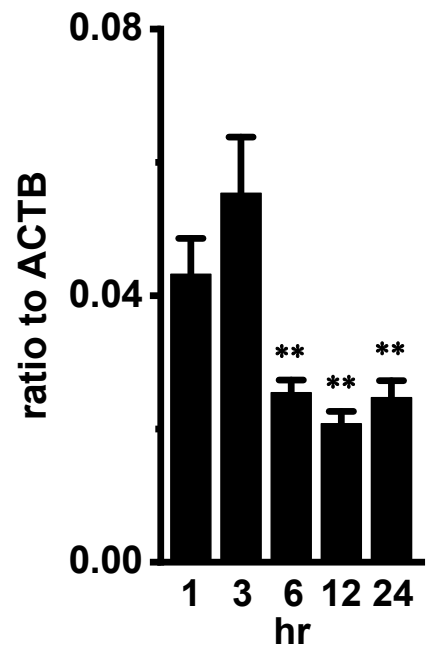
A. vehicle



B. DCEBIO

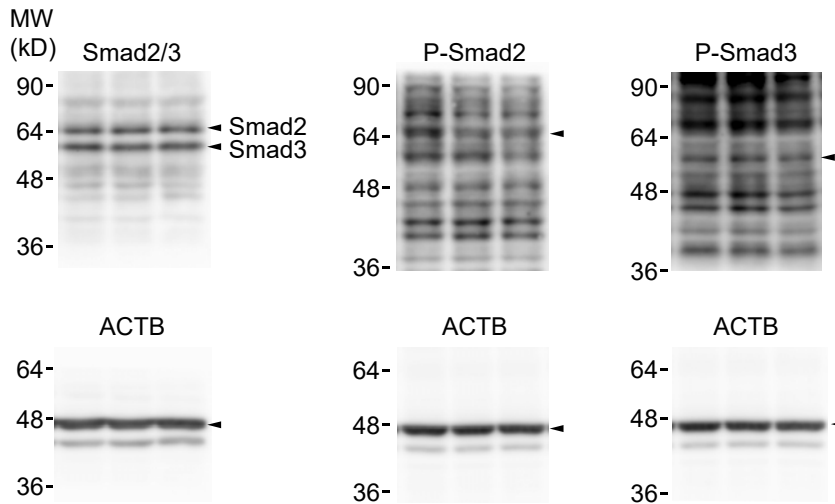


C. SKA-31

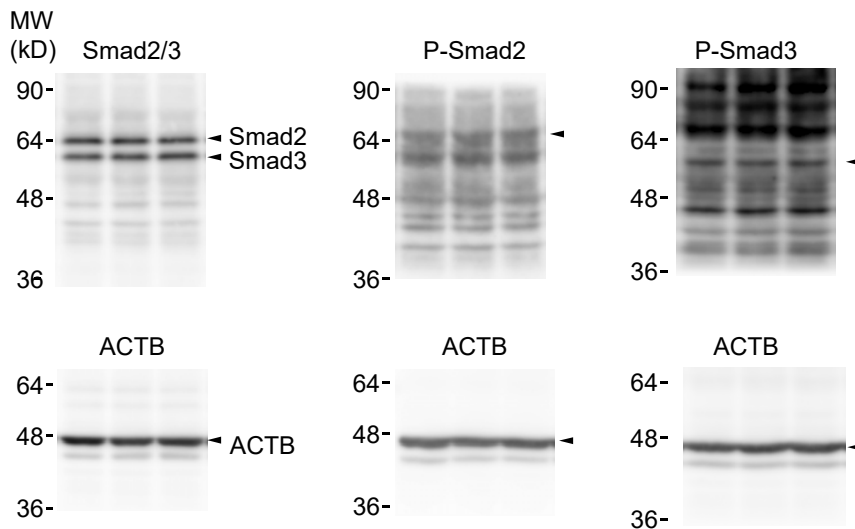


supplementary Fig. S5

A. full images of cropped blots shown in Figure 4

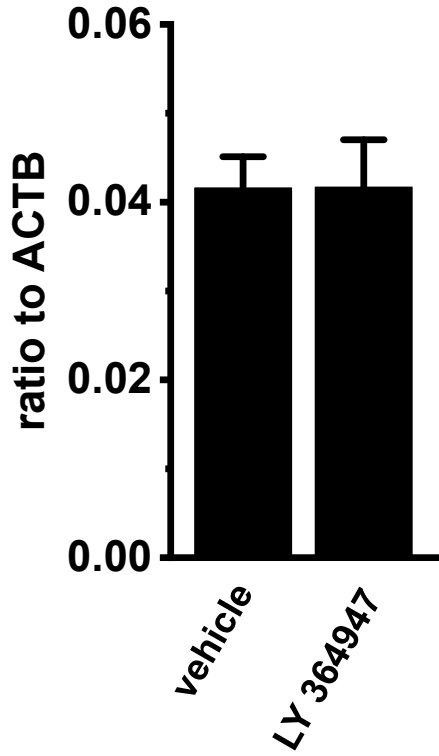


B. full images of cropped blots shown in Figure 7

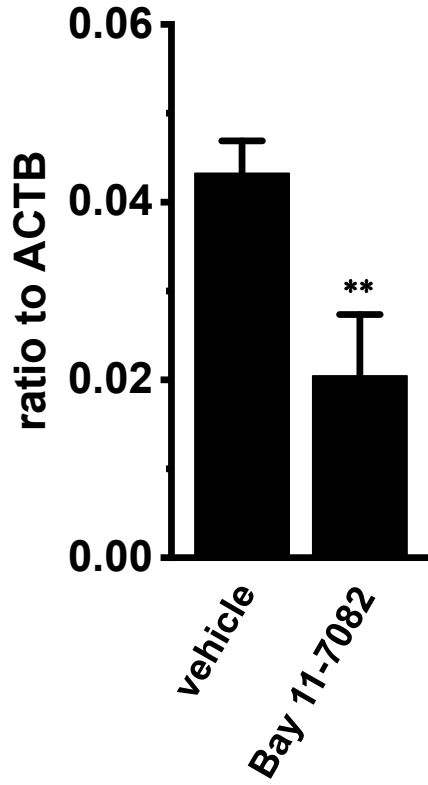


supplementary Fig. S6

A



B



C

